JCI The Journal of Clinical Investigation

Mechanism of rhinovirus-induced changes in airway smooth muscle responsiveness.

H Hakonarson, N Maskeri, C Carter, R L Hodinka, D Campbell, M M Grunstein

J Clin Invest. 1998;102(9):1732-1741. https://doi.org/10.1172/JCI4141.

Research Article

An important interplay exists between specific viral respiratory infections and altered airway responsiveness in the development and exacerbations of asthma. However, the mechanistic basis of this interplay remains to be identified. This study addressed the hypothesis that rhinovirus (RV), the most common viral respiratory pathogen associated with acute asthma attacks, directly affects airway smooth muscle (ASM) to produce proasthmatic changes in receptor-coupled ASM responsiveness. Isolated rabbit and human ASM tissue and cultured ASM cells were inoculated with human RV (serotype 16) or adenovirus, each for 6 or 24 h. In contrast to adenovirus, which had no effect, inoculation of ASM tissue with RV induced heightened ASM tissue constrictor responsiveness to acetylcholine and attenuated the dose-dependent relaxation of ASM to beta-adrenoceptor stimulation with isoproterenol. These RV-induced changes in ASM responsiveness were largely prevented by pretreating the tissues with pertussis toxin or with a monoclonal blocking antibody to intercellular adhesion molecule-1 (ICAM-1), the principal endogenous receptor for most RVs. In extended studies, we found that the RV-induced changes in ASM responsiveness were associated with diminished cAMP accumulation in response to dose-dependent administration of isoproterenol, and this effect was accompanied by autologously upregulated expression of the Gi protein subtype, Gialpha3, in the ASM. Finally, in separate experiments, we found that the RV-induced effects on ASM responsiveness were also accompanied by autologously induced upregulated […]

Mechanism of Rhinovirus-induced Changes in Airway Smooth Muscle Responsiveness

Hakon Hakonarson, Neil Maskeri, Carrie Carter, Richard L. Hodinka,* Donald Campbell,* and Michael M. Grunstein
*Division of Pulmonary Medicine and *Division of Immunologic and Infectious Diseases, Joseph Stokes, Jr. Research Institute, The Children's Hospital of Philadelphia, University of Pennsylvania School of Medicine, Philadelphia, Pennsylvania 19104*

Abstract

An important interplay exists between specific viral respiratory infections and altered airway responsiveness in the development and exacerbations of asthma. However, the mechanistic basis of this interplay remains to be identified. This study addressed the hypothesis that rhinovirus (RV), the most common viral respiratory pathogen associated with acute asthma attacks, directly affects airway smooth muscle (ASM) to produce proasthmatic changes in receptor-coupled ASM responsiveness. Isolated rabbit and human ASM tissue and cultured ASM cells were inoculated with human RV (serotype 16) or adenovirus, each for 6 or 24 h. In contrast to adenovirus, which had no effect, inoculation of ASM tissue with RV induced heightened ASM tissue constrictor responsiveness to acetylcholine and attenuated the dose-dependent relaxation of ASM to β-adrenoceptor stimulation with isoproterenol. These RV-induced changes in ASM responsiveness were largely prevented by pretreating the tissues with pertussis toxin or with a monoclonal blocking antibody to intercellular adhesion molecule-1 (ICAM-1), the principal endogenous receptor for most RVs. In extended studies, we found that the RV-induced changes in ASM responsiveness were associated with diminished cAMP accumulation in response to dose-dependent administration of isoproterenol, and this effect was accompanied by autologously upregulated expression of the G_i protein subtype, $G_i\alpha_3$, in the ASM. Finally, in separate experiments, we found that the RV-induced effects on ASM responsiveness were also accompanied by autologously induced upregulated mRNA and cell surface protein expression of ICAM-1. Taken together, these findings provide new evidence that RV directly induces proasthmatic phenotypic changes in ASM responsiveness, that this effect is triggered by binding of RV to its ICAM-1 receptor in ASM, and that this binding is associated with the induced endogenously upregulated expression of ICAM-1 and enhanced expression and activation of G_i protein in the RV-infected ASM. (*J. Clin. Invest.* 1998. 102:1732–1741.) Key words: airway smooth muscle • rhinovirus infection • β-adrenergic stimulation • intercellular adhesion molecule-1 • asthma

Introduction

It is clinically well established that most children and young adults who develop asthma have elevated serum IgE levels, a history of early viral respiratory infections, and exacerbations of their asthma by recurrent viral respiratory illnesses (1, 2). A transient airway hyperreactivity is also reported to occur in nonasthmatic subjects after infection with certain respiratory viral pathogens, notably including rhinovirus (RV),[1] respiratory syncytial virus, and parainfluenza virus (3–7). While the basic mechanism(s) underlying this transient airway hyperreactivity or exacerbation of asthma symptoms remains to be established, recent evidence supports the general concept that the airway responses in asthma and to specific viral respiratory pathogens, including airways inflammation (8, 9), cytokine release (10, 11), and IgE production (12, 13), may share certain common mechanistic pathways. Moreover, within the broader context of the pathobiology of airway hyperreactivity and asthma, an important mechanistic association has been established between the presence of airway inflammation and the phenotypic changes in airway function that characterize the asthmatic state, including enhanced airway smooth muscle (ASM) constrictor responsiveness and impaired ASM relaxation responsiveness to β-adrenergic receptor stimulation (14–16). This association has been inferred from a host of clinical studies, as well as investigations incorporating various experimental animal models that express the proasthmatic phenotype. Accordingly, altered airway responsiveness has been reported after the administration of different proinflammatory agents into the lung including sensitizing antigens, ozone inhalation, activated leukocyte products, and chemotactic factors (17, 18), in addition to the instillation of various viral respiratory pathogens (19, 20). Collectively, these studies suggest a complex interrelationship between specific viral respiratory pathogens, activated inflammatory cells, airway epithelial cells, and altered ASM function.

Although the cellular and molecular mechanisms underlying the above fundamental changes in ASM responsiveness after viral respiratory infections remain largely unidentified, it is relevant to note that recent reports have demonstrated airway

Address correspondence to Michael M. Grunstein, M.D., Ph.D., Division of Pulmonary Medicine, The Children's Hospital of Philadelphia, University of Pennsylvania School of Medicine, 34th Street and Civic Center Boulevard, Philadelphia, PA 19104. Phone: 215-590-3497; FAX: 215-590-1397; E-mail: grunstein@email.chop.edu

Received for publication 29 May 1998 and accepted in revised form 3 September 1998.

J. Clin. Invest.

0021-9738/98/11/1732/10 $2.00
Volume 102, Number 9, November 1998, 1732–1741
http://www.jci.org

1. *Abbreviations used in this paper:* ACh, acetylcholine; ASM, airway smooth muscle; CPE, cytopathic effects; GAPDH, glyceraldehyde phosphate dehydrogenase; HBSM, human bronchial smooth muscle; ICAM-1, intercellular adhesion molecule-1; PECAM-1, platelet endothelial cell adhesion molecule-1; PT, pertussis toxin; Rmax, maximum relaxation; RV, rhinovirus; SmBM, smooth muscle basal medium; Tmax, maximum contraction; TSM, tracheal smooth muscle.

hyperresponsiveness to receptor-coupled constrictor agonists in both human (5–7, 20–23) and animal (24–29) airways that have been inoculated with specific viral respiratory pathogens. Moreover, impaired relaxation responsiveness to β-adrenoceptor stimulation in proasthmatic isolated airways has also been observed in ASM tissues preconstricted with a muscarinic-cholinergic agonist or histamine, and not in tissues contracted with the non–receptor-coupled constrictor agent, KCl (30–33). Taken together, these findings suggest that the changes in ASM responsiveness in the proasthmatic state may be attributed to perturbations in certain key receptor-coupled transmembrane signal transduction processes that regulate ASM contraction and relaxation.

In light of the above considerations, together with our recent evidence implicating an induced autocrine role for the ASM itself in autologously producing its altered responsiveness in the proasthmatic atopic sensitized state (34), a phenomenon largely attributed to perturbed receptor/G protein–coupled transmembrane signaling (35, 36), this study addressed the hypothesis that specific viral respiratory pathogens can directly infect ASM and elicit proasthmatic perturbations in its agonist responsiveness. Accordingly, we examined whether RV, the most common viral respiratory pathogen associated with acute asthma attacks, induces changes in receptor-coupled ASM responsiveness and if this action of the respiratory viral pathogen on airway responsiveness is related to altered receptor/G protein–coupled transmembrane signaling in the ASM. The results provide new evidence demonstrating that (*a*) RV (serotype 16) can directly infect ASM and induce proasthmatic changes in ASM responsiveness, characterized by heightened constrictor responsiveness and impaired β-adrenoceptor–mediated relaxation; (*b*) this effect is triggered by binding of RV to its intercellular adhesion molecule-1 (ICAM-1) receptor in ASM; and (*c*) the latter is coupled to the upregulated expression of ICAM-1 and enhanced expression and activation of G_i protein (notably, $G_i\alpha_3$), which produces inhibition of adenylate cyclase activity in the RV-infected ASM. Collectively, these new findings implicate an endogenous role for the ASM in autologously inducing proasthmatic changes in ASM responsiveness after RV infection.

Methods

Animals. Adult New Zealand White rabbits were used in this study approved by the Biosafety and Animal Research Committee of the Joseph Stokes Research Institute at Children's Hospital of Philadelphia. The animals had no signs of respiratory disease for several weeks before the study.

Culture of respiratory viruses. Virus stock solutions were generated by infecting monolayer cultures of sensitive cell systems with freshly isolated respiratory viruses by the Clinical Virology Laboratory at the Children's Hospital of Philadelphia, including human RV and adenovirus. In addition, human RV serotype 16 was purchased from the American Type Culture Collection (Rockville, MD) and cultured in the laboratory. Human embryonic lung fibroblasts (MRC-5) were used to culture the RV, and human carcinoma cells from lung (A549) were used to culture adenovirus. The cultures were grown in modified Eagle's minimum essential medium supplemented with Earle's balance salt solution, 1% L-glutamine, 7.5% FBS, Hepes buffer, and antimicrobial agents (5 μg/ml gentamicin, 10 μg/ml vancomycin, and 10 μg/ml amphotericin-B). When infection was notably advanced, as evidenced by obvious cytopathic effects (CPE), cell supernatants were harvested and frozen in aliquots ($\sim 2–4 \times 10^6$ virus particles/aliquot) at −70°C, as previously described (37), for use in the experiments described below.

Detection of respiratory viruses in ASM cells. Rabbit ASM cells cultured in the laboratory (see below) were propagated in 16 × 125 mm sterile plastic tissue culture using RPMI 1640 medium supplemented with 20% FBS, 10% L-glutamine, Hepes buffer, 200 U/ml of penicillin, and 200 μg/ml of streptomycin. Confluent monolayers of ASM cells were then separately inoculated with stock solutions ($\sim$ 1 million virus particles/T_{25} flask) of the above viruses. The culture tubes were maintained in slanted stationary racks at 33°C for 14 d and examined daily for viral-induced CPE, as demonstrated by the presence of various sizes of rounded refractile cells with lytic lesions. The cell culture supernatants were also salvaged at various times after infection and stored at −70°C for subsequent determination of viral content. Viral titers of the material used for infection and of the supernatants removed at the end of the infection period were also obtained to estimate the maximal amount of viral uptake that had occurred during the exposure period. Infection by adenovirus was confirmed using immunofluorescence staining of acetone-fixed infected cells, using mouse monoclonal antibodies directed against adenovirus, and a goat anti–mouse FITC conjugate. Due to the lack of commercially available antibodies to RV serotypes, detection of infection of the ASM cells with RV was confirmed by RT-PCR and Southern blotting. The PCR reactions were performed using cDNA reverse transcribed from total RNA isolated from ASM cells that were inoculated for 72 h with RV in the absence and presence of 1 h pretreatment with a monoclonal blocking antibody to ICAM-1 (4 μg/ml), using RV-specific primer pairs (i.e., 5-prime 5′-GCACTTCT-GTTTCCCC-3′; and 3-prime 5′-CGGACACCCAAAGTAG-3′) and a cDNA probe prepared by pooling, purifying, and sequencing the above PCR reactions.

Viral inoculation of ASM tissue. Our method for preparing rabbit ASM tissue has been described previously (36). In brief, after anesthesia with xylazine (10 mg/kg) and ketamine (50 mg/kg) the animals were killed with an intravenous overdose of pentobarbital (130 mg/kg). The tracheae were removed, cleaned of loose connective tissue, and divided into 6–8-mm ring segments. In comparable studies, human bronchial smooth muscle (HBSM) tissue was also obtained from patients undergoing lung resection for peripheral lung carcinoma and having no evidence of obstructive lung disease, as assessed by routine pulmonary function testing preoperatively. After lung resection, the specimens were macroscopically examined and, from tumor-free sites, bronchi (3–5 mm ID) from the third to fifth generation were dissected free from the surrounding parenchyma and sectioned into ring segments. Each alternate adjacent rabbit or human ASM ring segment was then incubated for 24 h at room temperature in Dulbecco's modified Eagles medium in the absence and presence of maximum effective concentrations ($\sim 10^6$ viral particles/ml) of either RV, adenovirus, or heat-inactivated RV (i.e., 65°C for 1 h) for 90 min at the optimal replication temperature for each virus. The viral inoculation experiments were conducted in the absence and presence of 1-h pretreatment with monoclonal blocking antibodies to the adhesion molecules, ICAM-1 (4 μg/ml) or platelet endothelial cell adhesion molecule-1 (PECAM-1; 4 μg/ml). In separate experiments, the above viral inoculations were performed in the absence and presence of 1 h of pretreatment with pertussis toxin (PT, 100 ng/ml), as previously described in our laboratory (36). The tissues were aerated with a supplemental oxygen mixture (95% O_2/5% CO_2) throughout the incubation period and, thereafter, the tissues' responsiveness to specific ASM constrictor and ASM relaxation agonists, second messenger accumulation, and G protein and ICAM-1 expression were examined, as described below.

Viral inoculation of cultured ASM cells. Rabbit ASM cells cultured in our laboratory have been characterized previously in detail with respect to their distinguishing morphological, histological, and immunological features (38). The cell isolation and subcultivation procedures were described previously (38). In brief, ASM cells were isolated from epithelium-denuded trachealis muscle from adult New

Zealand White rabbits. After digestion in F-12 containing 30 μg/ml protease, 55 μg/ml type IV collagenase, and 100 μg/ml trypsin inhibitor, the dissociated cells were centrifuged and resuspended in F-12 containing 10% FBS and 100 μg/ml of gentamicin sulfate. The cells were then inoculated in 100-mm tissue culture dishes and, after 4 wk, the cells had sufficiently proliferated to permit routine subcultivations. At weekly intervals, the subcultivated cells were suspended and then inoculated at a density of 10^4 cells/cm^2 in 75-cm^2 tissue culture flasks containing F-12 with 10% FBS and incubated at 37°C in a humidified atmosphere of 5% CO_2/95% air. When the cells were > 90% confluent, the original culture medium was replaced with Ham's F-12 for 24 h. The medium was then aspirated and the cells were inoculated, in separate experiments, with maximum effective concentrations ($\sim 10^6$ viral particles per T_{25} flask) of either RV, adenovirus, or heat-inactivated RV in 0.5 ml of culture media for 60 min at the optimal replication temperature for each virus in the absence and presence of a monoclonal blocking antibody to ICAM-1 (i.e., anti–ICAM-1 mAb). The cells were then washed once with fresh media and incubated at 37°C for various time points (i.e., 0, 3, 6, or 24 h). The cells were then prepared for detection of ICAM-1 mRNA and protein expression, as described below.

In parallel experiments, HBSM cells (Clonetics, San Diego, CA) derived from two healthy male donors, aged 16 and 21 yr, were grown in smooth muscle basal medium (SmBM) supplemented with 5% FBS, insulin (5 ng/ml), EGF (10 ng/ml), FGF (2 ng/ml), gentamicin (50 ng/ml), and amphotericin-B (50 ng/ml). The standard experimental protocol involved growing the cells to confluence in the above medium, then starving the cells in unsupplemented SmBM for 24 h, at which time the cells were treated with either RV or adenovirus in the absence and presence of anti–ICAM-1 mAb. The cellular RNA was harvested at the various time points and used for detection of ICAM-1 mRNA and protein expression as described below.

Pharmacodynamic measurements of ASM responsiveness. After incubation of the tissue preparations, each rabbit airway segment was suspended longitudinally between stainless steel triangular supports in siliconized 20-ml organ baths (Harvard Apparatus, Inc., South Natick, MA). The lower support was secured to the base of the organ bath, and the upper support was attached via a gold chain to a force transducer (FT.03C; Grass Instrument Co., Quincy, MA) from which isometric tension was continuously displayed on a multichannel recorder. Care was taken to place the membranous portion of the trachea between the supports in order to maximize the recorded tension generated by the contracting trachealis muscle. The tissues were bathed in modified Krebs-Ringer solution containing (mM): 125 NaCl, 14 $NaHCO_3$, 4 KCl, 2.25 $CaCl_2 \cdot H_2O$, 1.46 $MgSO_4 \cdot H_2O$, 1.2 $NaH_2PO_4 \cdot H_2O$, and 11 glucose. The baths were aerated with 5% CO_2 in oxygen; a pH of 7.35–7.40 was maintained, and the organ bath temperature was held at 37°C. Passive resting tension of each tracheal smooth muscle (TSM) segment was set at 2.0 *g* after the tissue had been passively stretched to a tension of 8 *g* in order to optimize the resting length of each segment, as previously described in our laboratory (39). The tissues were allowed to equilibrate in the organ baths for 45 min, at which time each tissue was primed with a 1-min exposure to 10^{-4} M acetylcholine (ACh). Cholinergic contractility was subsequently assessed in the TSM segments by cumulative administration of ACh in final bath concentrations ranging from 10^{-10} to 10^{-3} M. Thereafter, in separate studies, relaxation dose–response curves to isoproterenol (10^{-10} to 10^{-4} M) were conducted in tissues half-maximally contracted with ACh. The relaxant responses to isoproterenol were analyzed in terms of percent maximum relaxation (Rmax) from the initial level of active cholinergic contraction, and sensitivity to the relaxing agent was determined as the negative logarithm of the dose of isoproterenol producing 50% of Rmax (pD_{50}; i.e., geometric mean ED_{50} value).

Determination of cAMP accumulation. To determine whether β-adrenoceptor–mediated cAMP accumulation was altered by exposure of the ASM tissue to RV, isoproterenol-stimulated time-and dose-dependent changes in cAMP generation were assayed in RV-exposed (n = 4) and control (n = 4) tissues. For the time–response studies, TSM were isolated and prepared as described above, divided into separate segments, and each segment was exposed to isoproterenol (10^{-5} M) for 0, 0.5, 1, 2, 3, or 5 min. For the dose–response studies, the cAMP level was determined at 1 min after exposure of RV-treated and control TSM to varying concentrations of isoproterenol (10^{-7} to 10^{-4} M). In all the experiments, the tissues were treated with the phosphodiesterase inhibitor, 3-isobutyl-1-methylxanthine (IBMX; 10^{-5} M) for 30 min before isoproterenol administration. In these studies, after homogenization of the tissues, cAMP generation was determined using a commercially available radioimmunoassay, with [^{3}H]cAMP as tracer (Amersham International, Little Chalfont, UK). The tissues' protein concentration was assayed using the Lowry method, and the cAMP measurements were expressed in units of picomoles per milligram of tissue membrane protein.

Determination of G_i protein expression. Expression of the inhibitory G_i protein and its α subunits was assayed by Western blot analysis of membrane protein samples isolated from both RV-treated (n = 4) and control (n = 4) rabbit TSM tissue. The membrane protein samples were prepared as follows: trachealis muscle was minced and homogenized using a Wheaton Dounce tissue grinder in 40 vol of 50 mM Tris-HC1, 150 mM NaCl, 1 mM EDTA (pH 7.4) containing 1 mM phenylmethylsulfonyl fluoride, 5 μg/ml aprotinin, and 5 μg/ml leupeptin. Nuclei and large particulates were removed by centrifugation at 100 *g* for 5 min. The supernatant was then centrifuged at 100,000 *g* for 1 h to pellet the membrane fractions. The membrane pellet was resuspended in the same Tris-EDTA buffer, and the protein concentration was measured using the Lowry assay. Equivalent amounts (30–50 μg) of membrane protein were fractionated in 11% SDS-polyacrylamide gels followed by transfer to nitrocellulose membranes. The membranes were then blotted overnight at room temperature in 25 mM Tris-HCl (pH 7.5), 150 mM NaCl, and 0.05% Tergitol NP-40 containing 5% nonfat milk. The rabbit polyclonal anti–G_i-common, $G_i\alpha_1$, $G_i\alpha_2$, and $G_i\alpha_3$ antibodies were diluted at 1:1,000, 1:500, 1:500, and 1:500, respectively, and were incubated for 2 h at room temperature. The G_i-common antiserum recognizes $G_i\alpha_1$, $G_i\alpha_2$, and $G_i\alpha_3$ equivalently (40). The primary G_i antibodies were the generous gift of Dr. David Manning (University of Pennsylvania). All primary and secondary antibody incubations and washes were done in 25 mM Tris-HCl (pH 7.5), 150 mM NaCl, and 0.05% NP-40 containing 0.50% nonfat milk. The G_i proteins were detected using enhanced chemiluminescence (Amersham, Arlington Heights, IL) after a 1-h incubation with a 1:3,000 dilution of an anti–rabbit horseradish peroxidase–linked secondary antibody and subsequent exposure to autoradiography film. Expression levels of common and specific $G_i\alpha$-subunit proteins were quantitated using laser densitometry (Bio-Rad, Hercules, CA).

Determination of ICAM-1 expression in rabbit ASM cells by RT-PCR and Southern blot analysis. Total RNA was isolated from rabbit ASM cells in the absence and presence of exposure of the cells to RV for the various time points using the modified acid guanidinium thiocyanate phenol-chloroform extraction method to include proteinase K (in 0.5% SDS) digestion of protein in the initial RNA pellet (41). The concentration of each RNA sample was then determined spectrophotometrically. This procedure consistently yielded 15–20 μg of intact RNA per T-75 flask of ASM cells. To analyze the mRNA expression of ICAM-1, we used an RT-PCR protocol and ICAM-1 primers based on the published sequences of the human ICAM-1 gene, and included the following primer set: 5′-GAGCTGTTTGAGAACACCTC-3′ and 5′-TCACACTTCACTGTCACCTC-3′. Rabbit specific α-actin primers, 5′-CGACATCAAGGAGAAGCTG-3′ and 5′-CTAGAAGCATTTGCGGTGC-3′ (19 mers), based on the published sequence of the rabbit α-actin gene, were used to control for the transcription level of each sample. cDNA was synthesized using 2.5 μg of total RNA isolated from cells after 0, 3, 6, and 24 h of exposure to RV or media alone. The cDNA was primed with oligo(dT)12-18 and 2 μl of cDNA was used for each PCR reaction. The cycling profile used was as follows: denaturation: 95°C for 1 min; annealing: 56°C for 1.0 min; and extension: 72°C for 1 min and 34 cycles for the

ICAM-1 gene, and 24 cycles for the α-actin gene. The number of cycles was determined to be in the linear range of the PCR products. Equal aliquots of each PCR reaction were then run on a 1.2% agarose gel and subsequently transferred to a Zeta-probe membrane overnight in 0.4 N NaOH. After capillary transfer, the DNA was immobilized by UV cross-linking using a Stratalinker UV Crosslinker 2400 at 120,000 μJ/cm^2 (Stratagene, La Jolla, CA). Prehybridization in a Techne hybridization oven was conducted for 2–3 h at 42°C in 50% formaldehyde, 7% (wt/vol) SDS, 0.25 M NaCl, 0.12 M Na_2HPO_4 (pH 7.2), and 1 mM EDTA. Hybridization was for 20 h at 42°C in the same solution. The ICAM-1 and α-actin DNA levels were assayed by Southern blot analysis using ^{32}P-labeled probes, including the human-specific 3.3-kb ICAM-1 probe (American Type Culture Collection) ^{32}P-labeled in random primer reactions, and an α-actin probe prepared by pooling several RT-PCR reactions for the α-actin PCR fragments and purifying them from a 1.2% agarose gel using Qiaex II agarose gel extraction kit and then sequencing. Washes were as follows: 1 × 15 min in 2× SSC, 0.1% SDS; 1 × 15 min in 0.1× SSC, 0.1% SDS both at room temperature, and 2 × 15 min at 50°C in 0.1× SSC, 0.1% SDS. Southern blots were quantified by direct measurements of radioactivity in each band using a PhosphorImager (Molecular Dynamics, Sunnyvale, CA).

Determination of ICAM-1 expression in human ASM cells by Northern blot analysis. Total RNA was isolated from cultured human ASM cells, as described above. 15 μg of total RNA was fractionated in 1% agarose, 2.2 M formaldehyde denaturing gels, from cells initially maintained in SmBM media in the absence and presence of 0, 3, 6, and 24 h of exposure to RV. After capillary transfer to Zeta-probe membranes (Bio-Rad) in 10× SSC (1× SSC = 0.015 M sodium citrate), RNA was immobilized by UV cross-linking using a Stratalinker UV Crosslinker 2400 at 120,000 μJ/cm^2. Prehybridization in a hybridization oven was conducted for 2–3 h at 42°C in 50% formaldehyde, 7% (wt/vol) SDS, 0.25 M NaCl, 0.12M Na_2HPO_4 (pH 7.2), and 1 mM EDTA. Hybridization was for 20–22 h at 42°C in the same solution. The ICAM-1 mRNA levels were examined by Northern blot analysis using the human-specific 3.3-kb ICAM-1 probe, as described above. A human-specific probe for constitutively expressed glyceraldehyde phosphate dehydrogenase (GAPDH) was used as a control for RNA loading.

Determination of ICAM-1 expression in ASM cells and tissue by Western blot analysis. Expression of the cell surface adhesion molecule, ICAM-1, was assayed by Western blot analysis of membrane protein samples isolated from rabbit ASM tissue and human ASM cells in the absence and presence of a 24-h exposure to RV. The membrane protein samples were prepared as described above, and the membrane pellet was resuspended in Tris-EDTA buffer and the protein concentration was measured using the Lowry assay. Equivalent amounts (30 μg) of membrane protein were fractionated in 11% SDS-polyacrylamide gels followed by transfer to nitrocellulose membranes. The membranes were then blotted overnight in 25 mM Tris-HCl (pH 7.5), 150 mM NaCl, and 0.05% Tergitol NP-40 containing 5% nonfat milk, as described previously (36). The mouse anti–human ICAM-1 antibody used was diluted 1:500 and was then incubated for 1 h at room temperature. All primary and secondary antibody incubations and washes were done in 25 mM Tris-HCl (pH 7.5), 150 mM NaCl, and 0.05% NP-40 containing 0.50% nonfat milk. The ICAM-1 level was detected using enhanced chemiluminescence after a 1-h incubation with a 1:1,000 dilution of an anti–mouse horseradish peroxidase–linked secondary antibody and subsequent exposure to autoradiography film. Expression levels of ICAM-1 protein were quantitated using laser densitometry (Bio-Rad).

Determination of ICAM-1 expression in ASM cells by flow cytometry. ICAM-1 cell surface protein expression was also examined in the cultured rabbit ASM cells using a Coulter EPICS Elite flow cytometer (Coulter EPICS Division, Hialeah, FL) equipped with a 5-W argon laser operated at 488 nM and 300 mW output. Fluorescence signals were accumulated as two-parameter fluorescence histograms with both percent positive cells and mean channel fluorescence being recorded. Cells treated for 24 h in the absence and presence of either RV or adenovirus (see above) were carefully washed and then resuspended in PBS buffer, dispersed by pipetting and orbital shaking, and then stained with a mouse anti–human monoclonal antibody to ICAM-1. To examine for nonspecific binding, the primary antibody was replaced by Igs of the same isotype, following the manufacturer's protocol, using mouse IgG1 as a negative control. After serial washing, the cells were stained with FITC-conjugated goat anti–mouse secondary antibody. The antibody-stained cells were then evaluated by flow cytometry and analyzed using the Elite Immuno 4 statistical software (Coulter EPICS Division). Fluorescence intensities were expressed as percent positive cells, including mean channel fluorescence.

Statistical analysis. Unless otherwise indicated, results are expressed as mean±SE values. Statistical analysis was performed by means of the two-tailed paired Student's *t* test. $P < 0.05$ was considered significant.

Reagents. The human ICAM-1, rabbit α-actin, and RV-specific primers were obtained from Integrated DNA Technologies Inc. (Coralville, IA). ACh, isoproterenol hydrochloride, and ICAM-1 and PECAM-1 antibodies were obtained from Sigma Chemical Co. (St. Louis, MO). All drug concentrations are expressed as final bath concentrations. Isoproterenol and ACh were made fresh for each experiment, dissolved in normal saline to prepare 10^{-4} M and 10^{-3} M solutions, respectively. The human tissue was provided by the Cooperative Human Tissue Network which is funded by the National Cancer Institute.

Results

RV-induced changes in ASM responsiveness. Detection of infection of ASM cells by adenovirus was confirmed by evidence of CPE on days 7 and 14 after inoculation, using immunofluorescence staining of acetone-fixed infected cells with a mouse monoclonal antibody directed against adenovirus and a goat anti–mouse FITC conjugate (Fig. 1 *A*). Due to the lack of commercially available antibodies to RV serotypes, as shown in Fig. 1 *B*, infection of ASM cells with RV-16 was confirmed by RT-PCR and Southern blotting using RV-specific primer pairs (see Methods), and a cDNA probe prepared by purifying and sequencing the above PCR reactions. Moreover, in substantiating the specificity of the latter effect of RV exposure, in separate experiments, we found that pretreatment of ASM with a monoclonal blocking antibody to ICAM-1, the key cell surface receptor for the vast majority of RVs, prevented ASM infectivity by the virus (Fig. 1 *B*).

To examine the effects of viral infection on ASM responsiveness, in an initial series of experiments, airway constrictor and relaxation responses were separately examined in isolated TSM segments that were exposed to RV, adenovirus, or vehicle alone in the absence and presence of blockade of ICAM-1 with a monoclonal blocking antibody (anti–ICAM-1 mAb). In comparable experiments, we also used a monoclonal blocking antibody to PECAM-1 (anti–PECAM-1 mAb), the latter serving as a negative control. As shown in Fig. 2, relative to tissues incubated with control medium alone (*open circles*), the maximum contraction (Tmax) responses to ACh were significantly enhanced in TSM that were exposed to RV (*filled circles*). Accordingly, the mean±SE Tmax values amounted to 100.5±4.4 and 155.6±21.2 g/g TSM wt in the control and RV-exposed tissues, respectively ($P < 0.01$); and the corresponding pD_{50} (i.e., $-\log ED_{50}$) values averaged 4.39±0.05 and 5.03±0.20 −log M, respectively ($P < 0.05$). Moreover, it should be noted that these induced augmented constrictor responses to ACh were

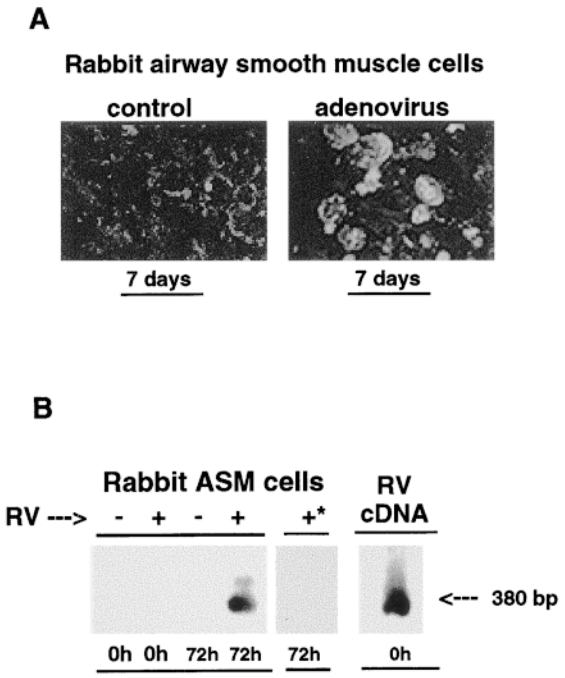

Figure 1. (*A*) Demonstration of viral antigen to adenovirus in rabbit ASM cells cultured in supplemented Eagle's minimum essential medium. Experimental cells (passages 6–8) were stained with virus-specific antibodies on day 7 of infection (see Methods). Note that viral antigen to adenovirus was readily detectable in infected cells which demonstrated classical CPE, as evidenced by the various sizes of rounded refractile cells with characteristic lytic lesions. (*B*) Southern blot of RV mRNA expression in rabbit ASM cells. Total RNA was isolated from cells inoculated for 72 h in the absence (−) and presence of RV exposure with (+*) and without (+) pretreatment with an anti–ICAM-1 mAb. RNA isolated from RV stock solution was used as a positive control (*RV cDNA*). The blot was probed with a sequenced ^{32}P-labeled cDNA probe prepared from pooled purified RT-PCR reactions for the RV gene. Note that in contrast to lack of expression in control (−) cells, RV mRNA expression was induced in RV-infected ASM cells at 72 h (+), and the latter was inhibited in the presence of anti–ICAM-1 mAb (+*).

largely prevented in the RV-exposed tissues that were pretreated with anti–ICAM-1 mAb (Fig. 2, *open squares*), wherein the mean±SE Tmax and pD_{50} values amounted to 119.6±14.9 g/g TSM wt and 4.43±0.07 −log M, respectively. There were no significant differences between the latter values and the corresponding determinations made in control tissues. In contrast to RV, exposure of ASM to adenovirus had no effect on the tissues' constrictor responsiveness to ACh (data not shown). Furthermore, in contrast to anti–ICAM-1 mAb, administration of anti–PECAM-1 mAb had no appreciable effect on the enhanced constrictor responsiveness to ACh obtained in RV-exposed TSM (data not shown).

In separate studies, during comparable levels of initial sustained ACh-induced contractions in RV-exposed and control airway segments, averaging ~ 45% of Tmax, administration of the β-adrenergic receptor agonist, isoproterenol, elicited cumulative dose-dependent relaxation of the precontracted TSM segments (Fig. 3). Relative to control TSM, however, the maximal relaxation responses (Rmax) and sensitivities (pD_{50} values) to isoproterenol were significantly attenuated in

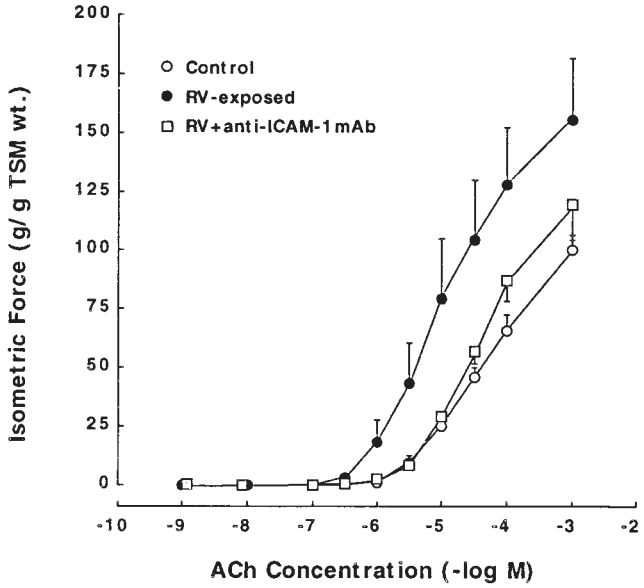

Figure 2. Comparison of constrictor dose–response relationships to ACh in control (*open circles*) and RV-exposed ASM in the absence (*filled circles*) and presence (*open squares*) of an anti–ICAM-1 mAb. Data are means±SE values. Note that both the Tmax and pD_{50} values to ACh are significantly enhanced ($P < 0.01$ and $P < 0.05$, respectively) in tissues exposed to RV, and that these effects of RV are largely inhibited in the presence of anti–ICAM-1 mAb.

the RV-exposed TSM. Accordingly, the mean Rmax values for isoproterenol amounted to 54.06±5.87% in the RV-exposed (Fig. 3, *filled circles*) tissues, compared with 69.12±4.85% in the control (*open circles*) TSM ($P < 0.05$); and the correspond-

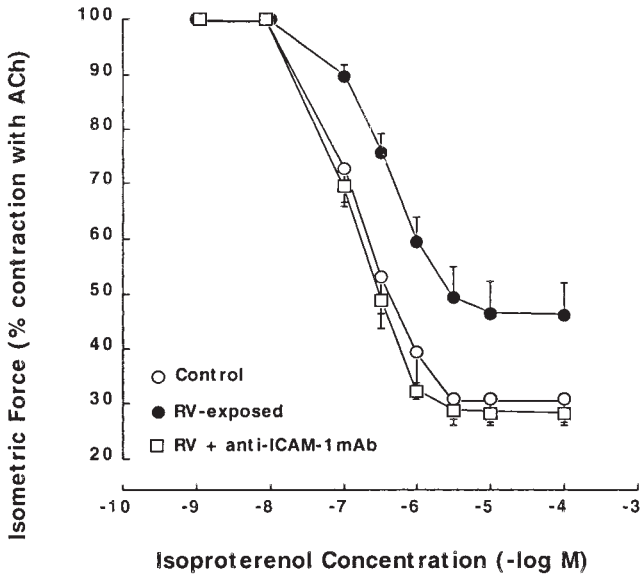

Figure 3. Comparison of relaxation response curves to isoproterenol in control (*open circles*) and RV-exposed ASM in the absence (*filled circles*) and presence (*open squares*) of an anti–ICAM-1 mAb. Data are means±SE values. Note that both the Rmax and pD_{50} values to isoproterenol are significantly attenuated ($P < 0.05$ and $P < 0.05$, respectively) in RV-exposed ASM, and that these effects of RV are largely inhibited in the presence of anti–ICAM-1 mAb.

ing pD_{50} values averaged 6.42±0.12 and 6.82±0.12 −log M, respectively ($P < 0.05$). As further depicted in Fig. 3 (*open squares*), the attenuated isoproterenol-induced relaxation responses were largely ablated in the RV-exposed TSM which were pretreated with anti–ICAM-1 mAb, wherein the mean Rmax value for isoproterenol amounted to 71.65±1.78% and the corresponding pD_{50} value averaged 6.89±0.05 −log M. There were no significant differences in either the Rmax or pD_{50} values between the control and RV-exposed tissues in the presence of anti–ICAM-1 mAb. In contrast to RV, exposure of ASM to adenovirus or initial heat inactivation of RV had no effect on the tissues' relaxant responsiveness to isoproterenol (data not shown). Moreover, in contrast to the action of anti–ICAM-1 mAb, administration of anti–PECAM-1 mAb to RV-exposed TSM had no effect on their impaired relaxation responses to isoproterenol (data not shown).

Altered cAMP accumulation in RV-exposed TSM. In light of the above observations, in comparable experiments, we examined whether the above attenuated isoproterenol-induced relaxation responses obtained in RV-exposed TSM were associated with altered β-adrenoceptor–coupled stimulation of cAMP accumulation, the key intracellular second messenger associated with ASM relaxation. Accordingly, the dose-dependent effects of isoproterenol on cAMP accumulation were compared in RV-exposed and control TSM segments. The mean (±SE) resting (baseline) levels of cAMP were similar in unstimulated control and RV-exposed TSM, averaging 5.5± 1.2 and 7.6±1.4 pmol/mg protein, respectively. In contrast, the peak increases in cAMP accumulation, determined at 1 min after each administered dose of isoproterenol, were significantly reduced in the RV-exposed tissues, as exemplified by a representative experiment comparing isoproterenol-induced cAMP accumulation in paired control and RV-exposed TSM (Fig. 4). Similar results were obtained in the other experiments ($n = 4$), wherein the collective mean maximal increases in cAMP accumulation in response to 10^{-5} M isoproterenol amounted to 2.45- and 1.45-fold above their respective baseline values in the control and RV-exposed TSM, respectively ($P < 0.05$).

Altered G_i protein expression and function in RV-exposed TSM. Given the above findings, together with our recent evidence that enhanced G_i protein expression and action underlies the attenuated relaxation responsiveness to isoproterenol in TSM passively sensitized with human atopic asthmatic serum (36), in separate experiments, we examined whether a similar mechanism pertains to our observed attenuated relaxation responses to isoproterenol in RV-exposed tissues. Accordingly, in initial pharmacodynamic studies, we investigated the effects of pretreatment of control and RV-exposed TSM with PT, which ADP-ribosylates G_i protein. Relative to control TSM, wherein PT had no effect, the Rmax and pD_{50} for isoproterenol were significantly enhanced in PT-treated versus untreated RV-exposed TSM (Fig. 5). Thus, the Rmax and pD_{50} values obtained in untreated RV-exposed tissues amounted to 36.02±7.13% and 6.17±0.19 −log M, respectively, compared with 68.15±4.2% and 6.42±0.07 −log M, respectively ($P < 0.05$), in the RV-exposed TSM that were pretreated with PT (Fig. 5). Of note, there were no differences in either the Rmax or pD_{50} values between control tissues (i.e., 74.78±11.24% and 6.53±0.17 −log M, respectively) and the RV-exposed tissues that were pretreated with PT. Thus, the attenuated isoproterenol-mediated TSM relaxation responses in RV-exposed tissues were ablated in the presence of PT, implicating a role for altered G_i protein–coupled function in mediating the impaired relaxation responses to β-adrenoceptor stimulation in RV-exposed TSM.

In view of the above pharmacodynamic evidence, we next examined whether the expression of G_i and its isoforms is modulated in plasma membranes isolated from RV-exposed TSM. Relative to controls, Western immunoblot analyses of

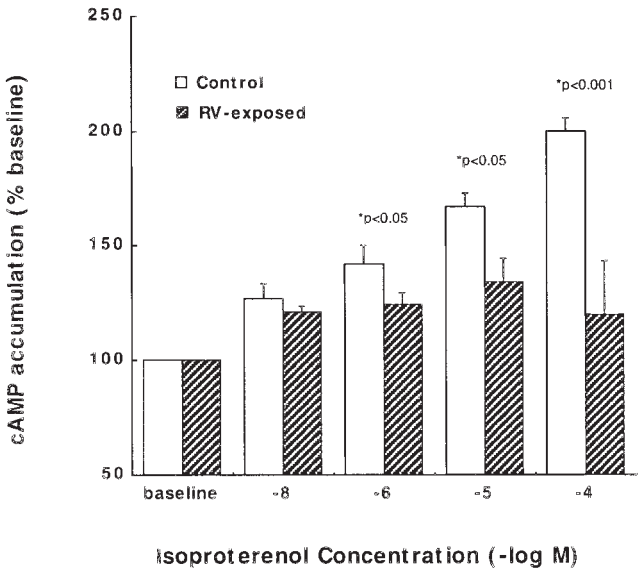

Figure 4. Comparison of isoproterenol-stimulated cAMP generation in paired control (*open bars*) and RV-exposed (*hatched bars*) TSM. Basal levels of cAMP were similar in both tissue groups, whereas the cAMP responses to isoproterenol stimulation were significantly reduced in the RV-exposed TSM. Data are means±SE values.

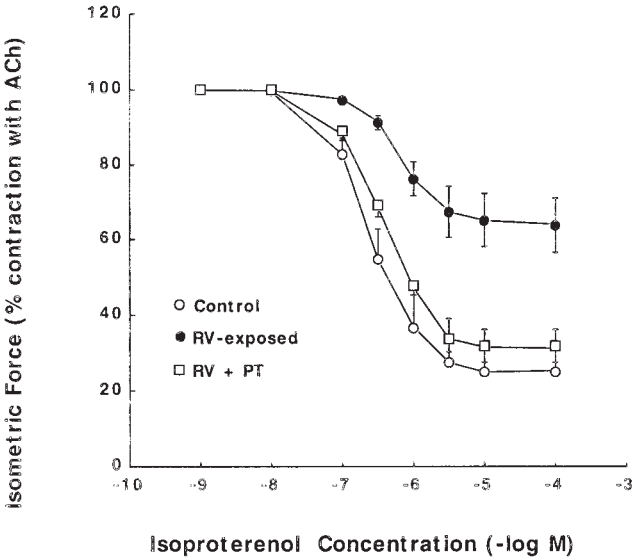

Figure 5. Comparison of relaxation response curves to isoproterenol in control (*open circles*) and RV-exposed ASM in the absence (*filled circles*) and presence (*open squares*) of PT. Data are means±SE values. Note that PT significantly enhanced both the Rmax ($P < 0.05$) and pD_{50} ($P < 0.05$) values to isoproterenol in RV-exposed ASM, and there were no differences in either the Rmax or pD_{50} values between control and RV-exposed tissues that were pretreated with PT.

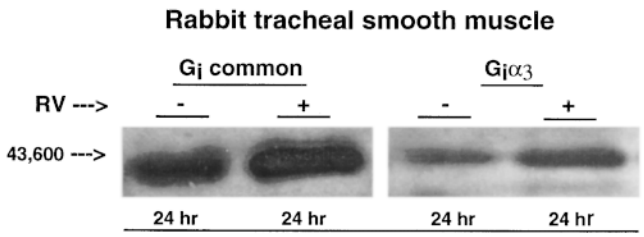

Figure 6. Comparison of Western blots of G_i-common (*left*) and $G_i\alpha_3$-subunit (*right*) expression in membrane homogenates prepared from control and RV-exposed TSM. Note enhanced expression of G_i-common and $G_i\alpha_3$ in sensitized compared with control samples.

G_i-common and specific $G_i\alpha$-subunit expression in membrane homogenates from RV-exposed TSM demonstrated increased levels of G_i-common and $G_i\alpha_3$, the latter quantified by laser densitometry at 3.3-fold ($P < 0.01$) and 2.2-fold ($P < 0.05$), respectively, above control values (Fig. 6). In contrast, neither $G_i\alpha_1$ nor $G_i\alpha_2$ expression was significantly different between control and RV-exposed TSM membrane fractions (data not shown).

Altered ICAM-1 expression in RV-exposed ASM. To the extent that RV-16 is a member of the major receptor group of RVs (constituting > 90% of RVs) which are known to exert their action by binding to their cell surface receptor, ICAM-1, we next examined whether ASM cells express ICAM-1 and whether expression of the latter is altered in the presence of RV. Accordingly, in initial studies, using RT-PCR and ICAM-1 specific primers, cDNA was reverse transcribed from total RNA isolated from rabbit ASM cells, primed with oligo(dT), and Southern blots were probed with a human cDNA probe specific for ICAM-1 (see Methods). A 415-bp α-actin probe was also used to control for gel loading, and the signals for the ICAM-1 and α-actin PCR products were quantified using a PhosphorImager. As demonstrated in Fig. 7, in contrast to the unaltered constitutive expression of α-actin, the ICAM-1 signal was significantly enhanced in cells that were exposed to RV, both at 6 and 24 h, whereas expression of ICAM-1 mRNA was essentially unaltered in control cells. Qualitatively similar results were obtained by Northern blot analysis of ICAM-1 mRNA expression in cultured HBSM cells that were exposed

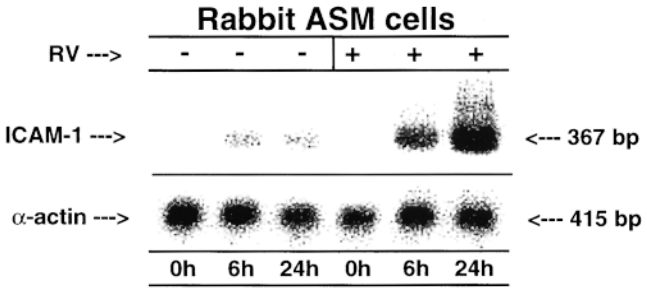

Figure 7. Southern blots of ICAM-1 and α-actin mRNA expression in rabbit ASM cells after 0, 6, and 24 h of inoculation in serum-free media in the absence (−) and presence (+) of RV. Note that in contrast to unaltered α-actin expression, expression of ICAM-1 was significantly induced at 6 and 24 h in cells that were exposed to RV. The blots were probed with sequenced ^{32}P-labeled cDNA probes prepared from pooled purified RT-PCR reactions for the human ICAM-1 and rabbit α-actin genes.

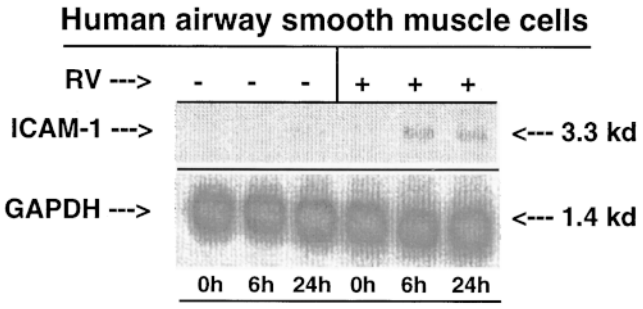

Figure 8. Representative Northern blot probed with human-specific ICAM-1 and GAPDH cDNA probes. Human ASM cells were incubated for 0, 6, and 24 h in culture media in the absence (−) and presence (+) of RV. 15 μg of RNA was loaded in each lane and run on a 1% agarose, 2.2% formaldehyde denaturing gel. Note that in contrast to unaltered GAPDH expression, ICAM-1 mRNA expression was upregulated at 6 and 24 h in cells that were exposed to RV.

to RV versus cell culture media alone (controls), as depicted in Fig. 8. Here, it should be noted that, in contrast to unaltered expression in control cells, the expression of ICAM-1 mRNA was significantly upregulated in the RV-exposed ASM cells for up to 24 h, whereas the mRNA levels for the constitutively expressed gene, GAPDH, were unaltered.

In extending the above observations, we subsequently examined whether HBSM cells express ICAM-1 on their cell surface, and whether the latter expression is modulated in the presence of RV. In one series of experiments, using Western blot analysis, we found that HBSM cells expressed ICAM-1 protein and that, in contrast to its unaltered expression in control cells, 24-h inoculation of cells with RV produced significantly enhanced expression of ICAM-1 protein, as exemplified in Fig. 9. Furthermore, in another complimentary series of experiments, we examined for altered ICAM-1 cell surface protein expression in cultured rabbit ASM cells after 24 h of inoculation with either RV or adenovirus. In concert with the above observations, our results demonstrated that, relative to control cells, ICAM-1 cell surface protein expression was significantly enhanced after 24 h of inoculation with RV (Fig. 10). Contrasting these results obtained with RV, inoculation of cells with adenovirus had no detectable effect on ICAM-1 expression (data not shown). Thus, taken together, these findings demonstrating enhanced ICAM-1 expression in RV-exposed ASM cells parallel the above observations implicating a role for ICAM-1 in mediating RV-induced changes in ASM responsiveness.

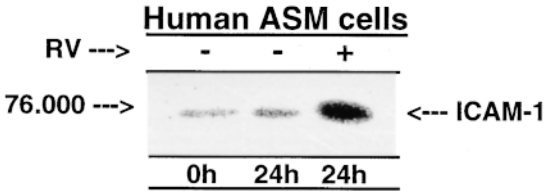

Figure 9. Representative Western blots depicting ICAM-1 expression in membrane homogenates from human ASM cells in the absence (−) and presence (+) of RV. 50 μg of protein was loaded in each lane. Note induced enhanced expression of ICAM-1 protein in cells that were exposed to RV.

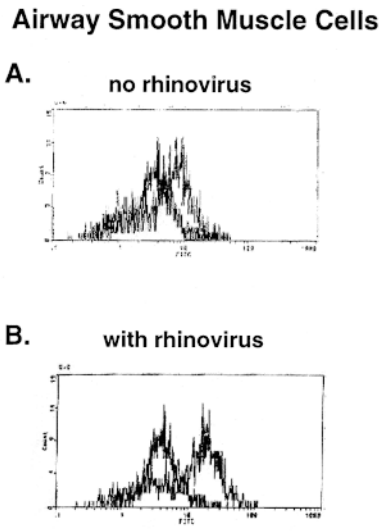

Figure 10. Representative flow cytometric analysis of ICAM-1 cell surface expression in control and RV-exposed ASM cells. Rabbit ASM cells were inoculated in serum-free media in the absence (*A*) and presence (*B*) of RV. The cells were stained with a mouse anti–human monoclonal antibody specific for ICAM-1. The levels of nonspecific background staining were measured by staining with FITC-conjugated isotype control IgG antibody (*left histogram*). Goat anti–mouse FITC-conjugated secondary antibody was used for detection of the signals. Note that relative to control cells (*A*) which demonstrated 32% positive staining for ICAM-1, cells treated with RV (*B*) demonstrated 69% positive staining for ICAM-1. In contrast, adenovirus had no effect on ICAM-1 expression (data not shown).

Discussion

Viral respiratory infections are associated with acute episodes of wheezing and asthma exacerbations throughout childhood. Beyond infancy, RV represents the predominant common cold virus that has been implicated in triggering acute wheezing in children and young adults. In this connection, it is relevant to note that RV infection has also been associated with elevation of serum total IgE levels (12, 13), increases in airway reactivity (5–7, 21–24), and increased eosinophil influx into the respiratory tract (4). A priori, when taken together, these effects of RV infection closely parallel the known proinflammatory changes in airway function observed in atopic asthma and, hence, suggest that a potentially important common mechanism underlies the perturbed airway function seen both in asthma and after RV infection. This study was designed, in part, to elucidate this mechanism. The results provide new evidence demonstrating that: (*a*) in contrast to adenovirus which has no effect, inoculation of naive ASM tissue with RV induces heightened ASM constrictor responsiveness and attenuated β-adrenoceptor–mediated ASM relaxation; (*b*) these RV-induced changes in ASM responsiveness are largely prevented by pretreating the tissues with PT or with a monoclonal blocking antibody to ICAM-1; (*c*) the RV-induced changes in ASM responsiveness are associated with attenuated cAMP accumulation in response to isoproterenol; (*d*) the latter is associated with the upregulated expression and action of the G_i protein subtype, $G_i\alpha_3$, in ASM; and (*e*) the above RV-induced changes in ASM responsiveness and G_i protein expression are accompanied by enhanced expression of ICAM-1, the principal receptor counterligand for RV.

Consistent with the above consideration of a potential common mechanism underlying the changes in airway function found in asthma and after RV infection, our present observations demonstrated that the altered ASM responsiveness seen in RV-exposed tissues was associated with perturbed receptor–coupled transmembrane signaling. In this regard, our present findings closely resemble those recently reported in isolated rabbit ASM passively sensitized with human atopic asthmatic serum, wherein we found that the induced proasthmatic changes in ASM responsiveness (i.e., increased contractility and attenuated relaxation) were largely attributed to the induced enhanced expression and action of G_i protein in the atopic asthmatic serum-sensitized state (36). Comparably, our present observations demonstrated that the impaired β-adrenoceptor–mediated relaxation of ASM inoculated with RV was largely prevented by pretreating the tissues with PT (Fig. 5), which ADP-ribosylates G_i protein, the latter mediating inhibition of adenylate cyclase activity. Furthermore, exposure of ASM to RV was found to upregulate G_i protein expression, specifically involving $G_i\alpha_3$ (Fig. 6). Thus, in considering our present findings, together with those previously reported in atopic asthmatic serum-sensitized ASM (36), it would appear that the attenuated β-adrenoceptor–coupled ASM relaxation observed in both atopic asthmatic serum-sensitized and RV-exposed ASM is largely attributed to enhanced G_i protein expression and function. Indeed, as demonstrated in Fig. 4, our observed upregulation of G_i protein expression and function was associated with reduced β-adrenoceptor–mediated accumulation of cAMP (Fig. 4). Although the specific regulatory mechanism underlying the change in G_i protein expression in RV-exposed ASM remains to be identified, it is potentially relevant to note that our earlier finding of enhanced G_i protein expression in atopic asthmatic serum-sensitized ASM was attributed to the induced autocrine release and action of the proinflammatory cytokine, IL-1β, by the ASM itself (34). Given the latter, and to the extent that infection with different viral respiratory pathogens (including RV) has been associated with the elaboration of various proinflammatory cytokines, including IL-1β (10, 11), the possibility is raised that our observed effects of RV on G_i protein expression may also be coupled to the induced autocrine release and action of specific cytokines affecting ASM transmembrane signaling. This possibility remains to be systematically investigated.

Apart from the effect of PT, our present observations demonstrated that the RV-induced changes in ASM responsiveness were also largely prevented by pretreating the tissues with anti–ICAM-1 mAb (Figs. 2 and 3). This finding implicates a role for ICAM-1 in mediating the RV-induced changes in ASM responsiveness. While more recently identified as the principal receptor for the vast majority (i.e., $> 90\%$) of RV subtypes (42, 43), ICAM-1 had been identified previously as the counterreceptor ligand for the β_2 integrin, lymphocyte function-associated antigen (LFA-1; CD11a/CD18). Accordingly, the binding of ICAM-1 to LFA-1, wherein expression of the latter is confined to leukocytes, has been demonstrated in a wide variety of cellular interactions, including T lymphocyte antigen-specific responses, leukocyte binding to endothelium, and emigration of leukocytes into inflammatory sites (44–47). In this context, the above role of ICAM-1 activation has been proposed in mediating the airway eosinophilia and hyperresponsiveness found in a primate model after chronic antigen challenge, as both the eosinophil influx and airway hyperresponsiveness were attenuated by administration of an anti–ICAM-1 antibody (48–50). Whereas the latter study implicated a role for ICAM-1 activation that is coupled to eosinophil influx in mediating changes in airway responsiveness, in a more recent study conducted on antigen-sensitized brown-Norway rats, an

anti–ICAM-1 antibody was found to reduce the airway constrictor hyperresponsiveness without producing a concomitant decrease in airway inflammation (51). Thus, although ICAM-1 activation may contribute to the development of airway hyperresponsiveness, the mechanism underlying this phenomenon may not be completely dependent on inflammatory cell influx. Indeed, in this regard, cell surface expression of ICAM-1 has been identified in a variety of cell types, including certain airway structural cells and smooth muscle cells (52–54). Moreover, expression of ICAM-1 on lung stromal cells and epithelial cells was found to be upregulated after exposure of asthmatic subjects to allergen (55, 56), and ICAM-1 expression was also reportedly increased in bronchial microvascular endothelial cells isolated from asthmatic individuals (57).

In light of the above evidence, our present observations, which demonstrate that RV-induced changes in ASM responsiveness are associated with ICAM-1 receptor activation and its upregulated expression in isolated ASM, suggest an important role for direct ICAM-1 activation on the surface of ASM cells in autologously mediating RV-induced changes in ASM responsiveness. The latter notion is consistent with the emerging general concept that, notwithstanding the established roles of infiltrating inflammatory cells and altered airway epithelial cell function in the pathogenesis of asthma, the ASM itself constitutes an autologously regulated system which, when activated in the sensitized state (e.g., after RV infection or atopic sensitization), induces its autologous expression of specific cell surface proteins (e.g., ICAM-1), as well as the autocrine release and action of specific cytokines (34), which lead to proasthmatic perturbations in ASM responsiveness. Furthermore, in relation to this concept, insofar as ICAM-1 activation is also crucial for immune effector cell mobilization, our finding of RV-induced upregulated ICAM-1 expression in ASM supports the notion of coexisting ICAM-1–coupled autologous mechanisms mediating both altered ASM responsiveness and localized airway inflammation in RV-infected ASM.

In conclusion, this study examined the role and mechanism of action of RV infection in isolated ASM on its agonist-mediated constrictor and relaxant responsiveness. The results demonstrated that: (*a*) inoculation of ASM with RV induces enhanced ASM constrictor responsiveness to ACh and impairs β-adrenoceptor–mediated ASM relaxation; (*b*) these effects of RV on ASM responsiveness are largely prevented by pretreating the ASM with PT, or with a monoclonal blocking antibody to ICAM-1; (*c*) the RV-induced changes in ASM responsiveness are associated with attenuated β-adrenoceptor–mediated stimulation of cAMP accumulation; (*d*) the latter is related to RV-induced upregulated expression of the G_i protein subtype, $G_i\alpha_3$; and (*e*) the above changes in ASM responsiveness and G_i protein expression are accompanied by RV-induced enhanced expression and action of ICAM-1 in ASM. Given the well-established clinical significance of RV infection in the pathogenesis of altered airway reactivity and asthma, the above findings of this study identify the important role and mechanism by which the ASM autologously induces its state of altered responsiveness after infection with RV.

Acknowledgments

The authors thank J. Grunstein, S. Chang, and S. Ling for their expert technical assistance, and Margaret Brown for assistance with typing the manuscript.

This work was supported in part by National Heart, Lung and Blood Institute grants HL-31467 and HL-58245, a Parker B. Francis Fellowship Award, and an Institutional Developmental Fund Award from the Joseph Stokes, Jr. Research Institute of the Children's Hospital of Philadelphia.

References

1. Stark, J.M., and F.M. Graziano. 1995. Lower airway responses to viruses. *In* Asthma and Rhinitis. W.W. Busse and S.T. Holgate, editors. Blackwell Scientific Publications, Boston, MA. 1229–1243.

2. Martinez, F.D., A.L. Wright, L.M. Taussig, C.J. Holberg, and W.J. Morgan. 1995. Asthma and wheezing in the first six years of life. The Group Health Medical Associates. *N. Engl. J. Med.* 332:133–138.

3. Phelan, P.D., L.I. Landau, and A. Olinsky. 1982. Respiratory Illness in Children. 2nd ed. Blackwell Scientific, Oxford. 34–37.

4. Bjornsdottir, U.S., and W.W. Busse. 1992. Respiratory infections and asthma. *Respir. Clin. N. Am.* 76:895–915.

5. Lemanske, R.F., E.C. Dick, C.A. Swenson, R.F. Vrtis, and W.W. Busse. 1989. Rhinovirus upper respiratory tract infection increases airway hyperreactivity and late asthmatic reactins. *J. Clin. Invest.* 83:1–10.

6. Busse, W.W. 1990. Respiratory infections: their role in airway responsiveness and the pathogenesis of asthma. *J. Allergy Clin. Immunol.* 85:671–683.

7. Busse, W.W. 1989. The relationship between viral infections and onset of allergic diseases and asthma. *Clin. Exp. Allergy.* 19:1–9.

8. Fraenkel, D.J., P.G. Bardin, G. Sanderson, F. Lampe, S.L. Johnston, and S.T. Holgate. 1995. Lower airways inflammation during rhinovirus colds in normal and asthmatic subjects. *Am. J. Respir. Crit. Care Med.* 151:879–886.

9. Bardin, P.G., S.L. Johnston, and P.K. Pattemore. 1992. Viruses as precipitants of asthma symptoms. II. Physiology and mechanisms. *Clin. Exp. Allergy.* 22:809–822.

10. Subauste, M.C., D.B. Jacoby, S.M. Richards, and D. Proud. 1995. Infection of a human respiratory epithelial cell line with rhinovirus. Induction of cytokine release and modulation of susceptibility to infection by cytokine exposure. *J. Clin. Invest.* 96:549–557.

11. Noah, T.L., and S. Becker. 1993. Respiratory syncytial virus-induced cytokine production by a human bronchial epithelial cell line. *Am. J. Physiol.* 265: L472–L478.

12. Bahna, S.L., C.A. Horwitz, M. Fiala, and D.C. Heiner. 1978. IgE response in heterophil-positive infectious mononucleosis. *J. Allergy Clin. Immunol.* 62:167–173.

13. Griffin, D.E., S.J. Cooper, R.L. Hirsch, R.T. Johnson, I. Lindo de Soriano, S. Roedenbeck, and A. Vaisberg. 1985. Changes in plasma IgE levels during complicated and uncomplicated measles virus infections. *J. Allergy Clin. Immunol.* 76:206–213.

14. McFadden, E.R., Jr. 1994. Asthma: morphologic-physiologic interactions. *Am. J. Respir. Crit. Care Med.* 150:523–526.

15. Goldie, R.G., D. Spina, P.J. Henry, K.M. Lulich, and J.W. Paterson. 1986. In vitro responsiveness of human asthmatic bronchus to carbachol, histamine, beta-adrenoceptor agonists and theophylline. *Br. J. Clin. Pharmacol.* 22: 669–676.

16. Szentivanyi, A. 1968. The beta-adrenergic theory of the atopic abnormality in bronchial asthma. *J. Allergy.* 42:203–232.

17. Smith, H. 1989. Animal models of asthma. *Pulm. Pharmacol.* 2:59–74.

18. Wanner, A. 1990. Utility of animal models in the study of human airway disease. *Chest.* 98:211–217.

19. Doyle, W.J., D.P. Skoner, P. Fireman, J.T. Seroky, I. Green, F. Ruben, D.R. Kardatzke, and J.M. Gwaltney. 1992. Rhinovirus 39 infection in allergic and nonallergic subjects. *J. Allergy Clin. Immunol.* 89:968–978.

20. Doyle, W.J., D.P. Skoner, J.T. Seroky, P. Fireman, and J.M. Gwaltney. 1994. Effect of experimental rhinovirus 39 infection on the nasal response to histamine and cold air challenges in allergic and nonallergic subjects. *J. Allergy Clin. Immunol.* 93:534–542.

21. Skoner, D.P., T.L. Whiteside, J.W. Wilson, W.J. Doyle, R.B. Herberman, and P. Fireman. 1993. Effect of rhinovirus 39 infection on cellular immune parameters in allergic and nonallergic subjects. *J. Allergy Clin. Immunol.* 92: 732–743.

22. Blair, H.T., S.B. Greenberg, P.M. Stevens, P.A. Bilunos, and R.B. Couch. 1976. Effects of rhinovirus infection on pulmonary function of healthy human volunteers. *Am. Rev. Respir. Dis.* 114:95–102.

23. Gern, J.E., and W.W. Busse. 1995. The effects of rhinovirus infections on allergic airway responses. *Am. J. Respir. Crit. Care Med.* 152:S40–S45.

24. Buckner, C.K., D.E. Clayton, A.A. Ain-Shoka, W.W. Busse, E.C. Dick, and P. Shult. 1981. Parainfluenza 3 infection blocks the ability of a beta adrenergic receptor agonist to inhibit antigen-induced contraction of guinea pig isolated airway smooth muscle. *J. Clin. Invest.* 67:376–384.

25. Folkerts, G., and F.P. Nijkamp. 1995. Virus-induced airway hyperresponsiveness. *Am. J. Respir. Crit. Care Med.* 151:1666–1674.

26. Lemen, R.J. 1990. Clues to the mechanism of virus-induced asthma from animal models. *Semin. Respir. Med.* 11:321–329.

27. Inoue, H., S. Horio, M. Ichinose, S. Ida, W. Hida, T. Takishima, K. Ohwada, and M. Homma. 1986. Changes in bronchial reactivity to acetylcholine with type C influenza virus in dogs. *Am. Rev. Respir. Dis.* 133:367–371.

28. Buckner, C.K., V. Songsiridej, E.C. Dick, and W.W. Busse. 1985. In vivo and in vitro studies on the use of the guinea pig as a model for virus-provoked airway hyperreactivity. *Am. Rev. Respir. Dis.* 132:305–310.

29. Saban, R., E.C. Dick, R.I. Rishleder, and C.K. Buckner. 1987. Enhancement by parainfluenza 3 infection of the contractile responses to substance P and capsaicin in airway smooth muscle of the guinea pig. *Am. Rev. Respir. Dis.* 136:586–591.

30. Wills-Karp, M., and M.I. Gilmore. 1993. Increased cholinergic antagonism underlies impaired beta-adrenergic response in ovalbumin sensitized guinea pigs. *J. Appl. Physiol.* 74:2729–2735.

31. Goldie, R.G., D. Spina, P.J. Henry, K.M. Lulich, and J.W. Paterson. 1986. In vitro responsiveness of human asthmatic bronchus to carbachol, histamine, beta-adrenoceptor agonists and theophylline. *Br. J. Clin. Pharmacol.* 22: 669–676.

32. Kelly, L.J., B.J. Undem, and G.K. Adams III. 1993. Antigen-induced contractin of guinea pig isolated pulmonary arteries and lung parenchyma. *J. Appl. Physiol.* 74:1563–1569.

33. Popa, V., J.S. Douglas, and A. Bouhuys. 1973. Airway responses to histamine, acetylcholine and propranolol in anaphylactic hypersensitivity in guinea pigs. *J. Allergy Clin. Immunol.* 51:344–351.

34. Hakonarson, H., D.J. Herrick, P. Gonzalez-Serrano, and M.M. Grunstein. 1997. Autocrine role of IL-1β in altered responsiveness of atopic asthmatic sensitized airway smooth muscle. *J. Clin. Invest.* 99:117–124.

35. Hakonarson, H., D.J. Herrick, P. Gonzalez Serrano, and M.M. Grunstein. 1996. Mechanism of cytokine-induced modulation of beta-adrenoceptor responsiveness in airway smooth muscle. *J. Clin. Invest.* 97:2593–2600.

36. Hakonarson, H., D.J. Herrick, and M.M. Grunstein. 1995. Mechanism of impaired beta-adrenoceptor responsiveness in atopic sensitized airway smooth muscle. *Am. J. Physiol. (Lung Cell. Mol. Physiol.).* 269:L645–L652.

37. Gleaves, C.A., R.L. Hodinka, S.L.G. Johnston, and E.M. Swierkosz. 1994. Cumulative techniques and procedures in clinical microbiology. *In* Laboratory Diagnosis of Viral Infections. E.J. Baron, editor. *Am. Soc. Microbiol.* Washington, DC. 1–35.

38. Noveral, J.P., and M.M. Grunstein. 1992. Role and mechanism of thromboxane-induced proliferation of cultured airway smooth muscle cells. *Am. J. Physiol. (Lung Cell. Mol. Physiol.).* 263:L555–L561.

39. Grunstein, M.M., S.T. Chuang, C.M. Schramm, and N.A. Pawlowski. 1991. Role of endothelin-1 in regulating rabbit airway contractility. *Am. J. Physiol. (Lung Cell. Mol. Physiol.).* 260:L75–L82.

40. Carlson, E.E., L.F. Brass, and D.R. Manning. 1989. Thrombin and phorbol esters cause the selective phosphorylation of a G protein other than Gi in human platelets. *J. Biol. Chem.* 264:13298–13305.

41. Chomczynski, P., and N. Sacchi. 1987. Single-step method of RNA isolation by acid guanidinium thiocyanate-phenol-chloroform extraction. *Anal. Biochem.* 162:156–159.

42. Greve, J.M., G. Davis, A.M. Meyer, C.P. Forte, S.C. Yost, C.W. Marlor, M.E. Kamarck, and A. McClelland. 1989. The major human rhinovirus receptor is ICAM-1. *Cell.* 56:839–847.

43. Uncapher, C.R., C.M. DeWitt, and R.J. Colonno. 1991. The major and minor group receptor families contain all but one human rhinovirus serotype. *Virology.* 180:814–817.

44. Pyszniak, A.M., C. Carpenito, and F. Takei. 1997. The role of LFA-1 (CD11a/CD18) cytoplasmic domains in binding to intercellular adhesion molecule-1 (CD54) and in postreceptor cell spreading. *Exp. Cell Res.* 233:78–87.

45. Springer, T.A., M. Dustin, T.K. Kishimoto, and S.D. Marlin. 1987. The lymphocyte function-associated LFA-1, CD2, and LFA-3 molecules: cell adhesion receptors of the immune system. *Annu. Rev. Immunol.* 5:223–252.

46. Simmons, D., M.W. Makgoba, and B. Seed. 1988. ICAM, an adhesion ligand of LFA-1, is homologous to the neural cells adhesion molecule NCAM. *Nature.* 331:624–627.

47. Staunton, D.E., S.D. Marlin, C. Stratowa, M.L. Dustin, and T.A. Springer. 1988. Primary structure of ICAM-1 demonstrates interaction between members of the immunoglobulin and integrin. *Cell.* 52:925–933.

48. Wegner, C.D., R.H. Gundel, P. Reilly, N. Haynes, L.G. Letts, and R. Rothlein. 1990. Intercellular adhesion molecule-1 (ICAM-1) in pathogenesis of asthma. *Science.* 247:456–459.

49. Gundel, R.H., C.D. Wegner, C.A. Torcellini, and L.G. Letts. 1992. The role of intercellular adhesion molecule-1 in chronic airway inflammation. *Clin. Exp. Allergy.* 22:569–575.

50. Chin, J.E., G.E. Winterrowd, C.A. Hatfield, J.R. Brashler, R.L. Griffin, S.L. Vonderfecht, K.P. Kolbasa, S.F. Fidler, K.L. Shull, R.F. Krzesicki, et al. 1998. Involvement of intercellular adhesion molecule-1 in the antigen-induced infiltration of eosinophils and lymphocytes into the airways in a murine model of pulmonary inflammation. *Am. J. Respir. Cell Mol. Biol.* 18:158–167.

51. Sun, J., W. Elwood, A. Haczku, P.J. Barnes, P.G. Hellewell, and K.F. Chung. 1994. Contribution of intercellular-adhesion molecule-1 in allergen-induced airway hyperresponsiveness and inflammation in sensitised brown-Norway rats. *Int. Arch. Allergy Immunol.* 104:291–295.

52. Patel, J.A., M. Kunimoto, T.C. Sim, R. Garofalo, T. Elliott, S. Baron, O. Ruuskanen, T. Chonmaitree, P.L. Ogra, and F. Schmalstieg. 1995. Interleukin-1α mediates the enhanced expression of intercellular adhesion molecule-1 in pulmonary epithelial cells infected with respiratory syncytial virus. *Am. J. Respir. Cell Mol. Biol.* 13:602–609.

53. Tosi, M.F., J.M. Stark, A. Hamedani, C.W. Smith, D.C. Gruenert, and Y.T. Huang. 1992. Intercellular adhesion molecule-1 (ICAM)-1-dependent and ICAM-1 independent adhesive interactions between polymorphonuclear leukocytes and human airway epithelial cells infected with parainfluenza virus type 2. *J. Immunol.* 149:3345–3349.

54. Lazaar, A.L., H.E. Reitz, R.A. Panettieri, Jr., S.P. Peters, and E. Pure. 1997. Antigen receptor-stimulated peripheral blood and bronchoalveolar lavage-derived T cells induce MHC class II and ICAM-1 expression on human airway smooth muscle. *Am. J. Respir. Cell Mol. Biol.* 16:38–45.

55. Gosset, P., I. Tillie-Leblond, A. Janin, C.-H. Marguette, M.C. Copin, B. Wallaert, and A.B. Tonnel. 1995. Expression of E-selectin, ICAM-1 and VCAM-1 on bronchial biopsies from allergic and nonallergic asthmatic patients. *Int. Arch. Allergy Immunol.* 106:69–77.

56. Manolitsas, N.D., C.J. Trigg, A.E. McAulay, J.H. Wang, S.E. Jordan, A.J. D'Ardenne, and R.J. Davies. 1994. The expression of intercellular adhesion molecule-1 and the B1-integrins in asthma. *Eur. Respir. J.* 7:1439–1444.

57. Bentley, A.M., S.R. Durham, D.S. Robinson, G. Menz, C. Storz, O. Cromwell, A.B. Kay, and A.J. Wardlaw. 1993. Expression of endothelial and leukocyte adhesion molecules intercellular adhesion molecule-1, E-selectin, and vascular cell adhesion molecule-1 in the bronchial mucosa in steady-state and allergen-induced asthma. *J. Allergy Exp. Immunol.* 92:857–868.